Tests of the continuum limit for the SO(4) principal chiral model and the prediction for $\Lambda_{\overline{\rm MS}}$

M. Hasenbusch and R. R. Horgan
D.A.M.T.P., Silver Street, Cambridge CB3 9EW, England
(Received 7 November 1995)

We investigate the continuum limit in SO(N) principal chiral models concentrating in detail on the SO(4) model and its covering group SU(2)⊗SU(2). We compute the mass gap in terms of $\Lambda_{\overline{\rm MS}}$ and compare with the prediction of Hollowood of $m/\Lambda_{\overline{\rm MS}}=3.8716$. We use the finite-size scaling method of Lüscher, Weisz, and Wolff to deduce $m/\Lambda_{\overline{\rm MS}}$ and find that for the SO(4) model the computed result of $m/\Lambda_{\overline{\rm MS}}\sim 14$ is in strong disagreement with theory but that a similar analysis of the SU(2)⊗SU(2) model yields excellent agreement with theory. We conjecture that for SO(4) violations of the finite-size scaling assumption are severe for the values of the correlation length ξ investigated and that our attempts to extrapolate the results to zero lattice spacing, although plausible, are erroneous. Conversely, the finite-size scaling violations in the SU(2)⊗SU(2) simulation are consistent with perturbation theory and the computed β function agrees well with the three-loop approximation for couplings evaluated at scales $L/a\leqslant\xi$, where ξ is measured in units of the lattice spacing a. We conjecture that lattice vortex artifacts in the SO(4) model are responsible for delaying the onset of the continuum limit until much larger correlation lengths are achieved notwithstanding the apparent onset of scaling. Results for the mass spectrum for SO(N), $N=8,10$ are given whose comparison with theory gives plausible support to our ideas. [S0556-2821(96)06609-X]

PACS number(s): 11.15.Ha, 05.50.+q, 11.10.Lm, 64.60.Fr

I. INTRODUCTION

For many years the study of two-dimensional non-Abelian chiral models based on the manifold $M=G/H$, where G and H are Lie groups and $H\subset G$, has provided a deep understanding of field-theoretic methods applied to both high energy physics and critical phenomena. In particular, the continuum field theories derived from these models are renormalizable and asymptotically free and so act as good models to test ideas applicable to four-dimensional gauge theories. For many models the exact S matrix for the continuum field theory has been conjectured [3–5] and this allowed a number of workers [5–7] to give exact predictions for the mass spectrum and to use the thermodynamic Bethe ansatz together with the property of asymptotic freedom to predict the ratio $m/\Lambda_{\overline{\rm MS}}$ for these theories, where m is mass gap, $\Lambda_{\overline{\rm MS}}$ sets the mass scale in perturbation theory, and $\overline{\rm MS}$ denotes the modified minimal subtraction scheme. It is important to note that solely the local properties of M, i.e., the algebra which generates infinitesimal displacements on M, and not the global properties of M are used to obtain these results. To be able to control the approach to the continuum limit for a lattice field theory is central to current calculations in lattice QCD where criteria based on scaling are used to determine whether dimensionless ratios for computed observables have attained their continuum values and so can be compared with experiment. The existence of theoretical predictions for two-dimensional (2D) chiral field theories which link the short and long range structure of the theories gives a unique opportunity to study the approach to the continuum in a lattice model and also to test the assumptions underlying the theoretical analysis.

The correlation length is most conveniently measured in units of the lattice spacing, a, and is denoted by the dimensionless variable, ξ, and the mass gap is defined by $m=1/a\xi$. For ξ sufficiently large the mass spectrum inferred from the correlation functions of suitably chosen interpolating operators and the mass gap measured in units of $\Lambda_{\overline{\rm MS}}$ should agree with theory. Such agreement has been found for the SU(N) matrix models [8,9] for values of $N=3-15$ already for moderately small correlation lengths: $\xi>5$. However, the manifold of SU(N) is simply connected but this is not so for many other models for which it is important to see if any obstructions or lattice artifacts delay the onset of the continuum limit. We may then learn how to be more confident in controlling the approach to the continuum. Similarly good agreement with theory has also been found by Wolff [10] for the O(4) and O(8) spin models but not for the O(3) spin model [11,12]. A comparison of O(3) and RP^2 models has recently been the subject of much attention [13–17] since they are expected to correspond to the same continuum theory although they differ in the global properties of the defining manifolds. It has, however, proved impossible to demonstrate the equivalence of these two models in the continuum by computer simulation alone. The study reported in this paper highlights the difficulty of reliably controlling the approach to the continuum in a number of common lattice models.

We study the SO(N) matrix models on the lattice with the action given by

$$S(\mathbf{U})=\beta_L\sum_{x,t}\ \mathrm{Tr}[\mathbf{U}(x,t)\mathbf{U}^T(x,t+1)+\mathbf{U}(x,t)\mathbf{U}^T(x+1,t)], \tag{1.1}$$

where $\mathbf{U}(x,t)$ is an $N\times N$ orthogonal matrix. Our analysis mainly uses the finite size scaling method described by Lüscher *et al.* in Ref. [2]. For the lattice regularized theory we define the coupling constant $\tilde{u}$ by

$$\tilde{u}(L/a,\beta_L)=m(L/a,\beta_L)L, \tag{1.2}$$

where $m(L/a,\beta_L)$ is the mass gap, or inverse correlation length, measured on a lattice of spacing a, width L and infinite extension in time direction. In the simulation it suffices to take the extension in time direction $T \gg L$ to achieve this limit. The correlation length is determined by the decay of the correlation function on the $L \times T$ strip in the time direction. The physical properties can be separated from the cutoff dependence and the continuum coupling, $u(Lm_\infty)$, can be defined by writing

$$\tilde{u}(L/a,\beta_L) = \overline{u}(Lm_\infty, a/L) = u(Lm_\infty) + O((a/L)^\omega). \tag{1.3}$$

The physical scale is set by $m_\infty = 1/a\xi_\infty$, the mass gap in the infinite-volume limit. Apart from a trivial reparametrization, this decomposition relies on the physical hypothesis of scaling with the exponent ω parametrizing the corrections to scaling. For sufficiently large β_L and sufficiently small L/a perturbation theory can be used to compute u, and since it is proportional to $1/\beta_L$ at tree level it can be viewed as a definition for a running coupling of the continuum field theory. In particular u will evolve according to the universal part of the β function.

$u(Lm_\infty)$ can be calculated from a simulation of the lattice theory. For $Lm_\infty \geqslant 1$ this is straightforward: for a given value of β_L compute am_∞ and then simulate on a lattice of width L given in units of a by $L/a = Lm_\infty/am_\infty$, and so compute $\tilde{u}(L/a,\beta_L)$ from Eq. (1.2). Repeat for a sequence of β_L values, the largest of which is determined by computer resources. Check whether the results are compatible with the scaling hypothesis [Eq. (1.3)] and, if so, take $\overline{u}(Lm_\infty, a/L)$ with the largest L/a as the best approximation to $u(Lm_\infty)$ or, better still, use Eq. (1.3) to fit the a dependence and extrapolate to $a=0$.

However, this direct approach cannot be used for small values of Lm_∞ since $L/a \geqslant 1$ and am_∞ is bounded from below by computer resources and so limits how small Lm_∞ can be. This problem is resolved using the renormalization group by computing the lattice step-scaling function Σ:

$$\Sigma(s,\tilde{u}(L/a,\beta_L)) = \tilde{u}(sL/a,\beta_L). \tag{1.4}$$

Since no reference is made to m_∞ we can choose, for any given value of $\tilde{u}$, L/a as large as the computer resources will allow by tuning β_L appropriately. Again we expect the scaling hypothesis to hold:

$$\Sigma(s,\tilde{u}(L/a,\beta_L)) = \sigma(s,u) + O((a/L)^\omega). \tag{1.5}$$

$\sigma(s,u)$ is the continuum step-scaling function determined implicitly from the β function by

$$\ln(s) = -\int_u^{\sigma(s,u)} \frac{du'}{\beta(u')}. \tag{1.6}$$

The β function has the perturbative expansion

$$\beta(u) = -u^2 \sum_{l=0}^{\infty} b_l u^l. \tag{1.7}$$

Having computed $u(2)$, say, by the direct method a sequence of values $n_n \equiv u(2s^n)$ can be computed using

$$u_n = \sigma(s,u_{n-1}). \tag{1.8}$$

A reasonable choice for s is $s=1/2$. For couplings, u_n, evaluated at sufficiently large n, $\sigma(s,u)$ is well approximated by perturbation theory and Λ_ξ is given to two-loop order by

$$L\Lambda = [b_0 u(Lm_\infty)]^{-b_1/b_0^2} \exp\left(-\frac{1}{b_0 u(Lm_\infty)}\right), \tag{1.9}$$

where, for these theories, b_0 and b_1 are scheme independent. Hence m_∞/Λ_ξ is determined by substituting $Lm_\infty = 2s^n$. We have labeled Λ by ξ to denote this renormalization scheme: the ''ξ scheme.'' The coefficients b_0 and b_1 are scheme-independent (up to overall rescaling) and for some cases b_2 is known [2] yielding a three-loop estimate for Λ_ξ. A one-loop calculation then relates Λ_ξ to $\Lambda_{\overline{\rm MS}}$.

Alternatively, the approach used in Refs. [12,10,8,9] can be employed where a bare lattice coupling is defined to be a running coupling evaluated at the scale given by the lattice spacing, a. Two candidates are

$$u_L(am_\infty) = \frac{1}{\beta_L}: \quad \text{the ''lattice scheme,''} \tag{1.10}$$

$$u_E(am_\infty) = \frac{4\langle E\rangle}{C}: \quad \text{the ''energy scheme,''} \tag{1.11}$$

where $C = n_f$, n_f/N for spin and matrix models, respectively, and n_f is the number of degrees of freedom in the field. The coupling u_E was first defined by Parisi in Ref. [18]. For $\xi_\infty \gg 1$ both of these couplings should scale with a according to the perturbative β function thus allowing $a\Lambda_L$ and $a\Lambda_E$ to be computed from u_L and u_E, respectively, according to Eq. (1.9) with a replacing L. Since ξ_∞ is known this allows $m/\Lambda_{\overline{\rm MS}}$ to be estimated once the loop calculations relating $\Lambda_{\overline{\rm MS}}$ to Λ_L and Λ_E have been done. However, it should be noted that if such bare couplings are used then the effects of scaling violations cannot be disentangled.

The main motivation for our study was the recent work by Hollowood [1,19] in which he has given theoretical predictions for $m/\Lambda_{\overline{\rm MS}}$ for all $N>3$, so allowing us to compare our lattice calculations with theory. The comparison between the studies of the lattice and continuum models sheds light on the approach to the continuum limit in the lattice formulation and can provide verification of the assumptions underlying the theoretical analysis of the continuum theory. We calculate $\overline{u}(Lm_\infty, a/L)$ defined in Eq. (1.3) by simulation for various values of am_∞ and discuss the extrapolation of the results to $a=0$ and we repeat the analysis for the covering group of SO(4), namely SU(2)$\otimes$SU(2). We also compare the results with an analysis based on the lattice and energy schemes for the couplings defined in Eq. (1.11). For the SO(4) model we find no evidence that finite-size scaling holds for the accessible range of couplings, but that the results can deceptively suggest that it does hold since the violations of scaling diminish only slowly with increasing ξ so giving the semblance that they are negligible. In contrast, for SU(2)$\otimes$SU(2) finite-size scaling holds with O(a^2) violations and the value deduced for $m/\Lambda_{\overline{\rm MS}}$ agrees well with the prediction.

We also compare the computed mass spectrums in the SO(N) model for $N=8,10$ with theory. The interpolating fields for the vector bound states of SO(N) can be easily constructed and $N=8$ is the smallest value for which there exists more than one such state. The results show a persistent deviation from theory for the range of ξ investigated.

In Sec. II we present the relevant one-loop calculations which relate the various Λ parameters; in Sec. III we describe the simulation and measurement techniques including a method for variance reduction; in Sec. IV we give the simulation results and analysis for the study of the SO(4) matrix model; in Sec. V we give the simulation results for the SU(2)$\otimes$SU(2) model; in Sec. VI we discuss the $N=6,8,10$ models and compare the mass spectrum and $\Lambda_{\overline{\rm MS}}$, computed in the lattice and energy schemes, with theory; in Sec. VII we discuss our interpretation of all the results and how further studies may elucidate our findings. We also draw our conclusions.

II. THE ONE-LOOP CALCULATIONS RELATING DIFFERENT SCHEMES

A. SO(N)-matrix models

The energy scheme can be related to the lattice-scheme using the one-loop calculation for $\langle E\rangle$ expanded in $1/\beta_L \equiv u_L$. This calculation is familiar and we just give the result for general SO(N):

$$\langle E\rangle = \langle 1-(1/N)\ \mathrm{Tr}(\mathbf{U}(x,t)\mathbf{U}^T(x+1,t))\rangle.$$

$$= \frac{N-1}{8\beta_L}\left(1+\frac{N}{32\beta_L}+\cdots\right). \tag{2.1}$$

The energy-scheme coupling β_E is defined as

$$\beta_E = \frac{N-1}{8\langle E\rangle}, \tag{2.2}$$

and the ratio between Λ parameters is then

$$\frac{\Lambda_E}{\Lambda_L} = \exp\left(\frac{A}{b_0}\right)$$

$$= \exp\left(\frac{\pi N}{4(N-2)}\right), \tag{2.3}$$

where $\beta_E = \beta_L - A$.

A calculation similar to that described in Ref. [20] gives the result

$$\frac{\Lambda_{\overline{\rm MS}}}{\Lambda_L} = \sqrt{32}\exp\left(\frac{\pi N}{2(N-2)}\right). \tag{2.4}$$

Λ_ξ is related to Λ_L by a one-loop background field calculation in which the 2D theory on a strip is converted to a local 1D theory which can be directly solved for the mass gap since there is an equivalent Schrödinger equation. A similar approach was used in Ref. [21]. To analyze the 1D system it is sufficient to study the action

$$S(\mathbf{W}) = \beta_{\rm QM}\sum_t \mathrm{Tr}(\mathbf{W}_t\mathbf{W}_{t+1}). \tag{2.5}$$

We represent $\mathbf{W}$ by

$$\mathbf{W} = \exp(\phi\cdot\mathbf{T}),$$

where the generators T_i are defined so that

$$\mathrm{Tr}(T_iT_j) = -\frac{1}{2}\delta_{ij}. \tag{2.6}$$

Then for small ϕ we have

$$S(\phi) \sim \frac{\beta_{\rm QM}}{4}\sum_t \dot{\phi}^2 + \cdots .$$

This defines the quantum mechanics of a particle constrained to the SO(N) group manifold with mass $\mu=\beta_{\rm QM}/2$. The corresponding Schrödinger equation is then

$$-\frac{1}{2\mu}\mathbf{D}^2Y_l(\mathbf{W}) = E_lY_l(\mathbf{W}). \tag{2.7}$$

$\mathbf{D}$ is the group derivative [22] defined by

$$f(e^{\phi\cdot T}\mathbf{W}) = f(\mathbf{W}) + \phi\cdot\mathbf{D}f(\mathbf{W}) + \cdots .$$

The Y_l are group harmonics with l a generic label, and satisfy [22]

$$\mathbf{D}^2Y_l(\mathbf{W}) + C_lY_l(\mathbf{W}) = 0.$$

Using $Y_0\propto 1$ and $Y_1(\mathbf{W})\propto\mathrm{Tr}(\mathbf{W})$ we find $C_0=0$ and $C_1=C_F$, the Casimir of the fundamental representation deduced from the generators. From Eq. (2.6) we find

$$C_F = \frac{N-1}{4}$$

$$\Rightarrow$$

$$m(L) = \frac{E_1-E_0}{2\mu} = \frac{N-1}{4\beta_{\rm QM}}. \tag{2.8}$$

We now calculate $\beta_{\rm QM}$ in terms of β_L to one-loop order. The field variables $\mathbf{U}$ on the 2D strip of width L and length T can be expressed in terms of fluctuations about a background field $\mathbf{W_t}$ which is constant across the strip and slowly varying in t, the coordinate along the strip. We write

$$\mathbf{U}(x,t) = \mathbf{W}_t^{1/2}e^{g\phi(x,t)}\mathbf{W}_t^{1/2}, \tag{2.9}$$

where $\phi(x,t)\equiv\phi(x,t)\cdot\mathbf{T}$ is the fluctuation about $\mathbf{W}_t$. The definition of $\mathbf{W}_t$ is given by the relation

$$\sum_x \mathbf{U}(x,t) = \mathbf{W}_t^{1/2}\mathbf{S}_t\mathbf{W}_t^{1/2},$$

with $\mathbf{S}_t$ a positive symmetric matrix. Using Eq. (2.9) this corresponds at lowest order to the constraint

$$\sum_x \phi(x,t)=0. \tag{2.10}$$

Because $\mathbf{W}_t$ is slowly varying we can expand the effective 1D action in terms of Δ_t where $\Delta_t \equiv \mathbf{\Delta}_t \cdot \mathbf{T}$ and

$$\mathbf{W}_t \mathbf{W}_{t+1}^T = e^{\Delta t}.$$

To one-loop order this equation can be implemented by choosing

$$\mathbf{W}_t = 1 \quad \text{and} \quad \mathbf{W}_{t+1} = e^{-\Delta t}. \tag{2.11}$$

Substituting for $\mathbf{U}(x,t)$ and $\mathbf{W}_t$ from Eqs. (2.9) and (2.11) into the SO(N) action, Eq. (1.1), we find

$$S(\mathbf{U}) = \beta_L \sum_{x,t} \mathrm{Tr}(e^{g\phi(x,t)} e^{-g\phi(x+1,t)}) + \beta_L \sum_{x,t} \mathrm{Tr}(e^{g\phi(x,t)} e^{-\Delta_t/2} e^{-g\phi(x+1,t)} e^{-\Delta_t/2}). \tag{2.12}$$

Expanding to quadratic order, choosing $g^2 = 2/\beta_L$, and using Eq. (2.6), we find

$$S = S_0 + S_I,$$

where

$$S_0 = \sum_{x,t} \tfrac{1}{2} \phi \cdot \nabla \cdot \phi,$$

$$S_I = L\beta_L \sum_t -\tfrac{1}{2}\Delta_t \cdot \Delta_t + \sum_{x,t} \mathrm{Tr}(2\phi^2\Delta_t^2 + 2\phi'^2\Delta_t^2 - \phi'\phi\Delta_t^2 - \phi\phi'\Delta_t^2 - \phi\Delta_t\phi'\Delta_t). \tag{2.13}$$

The abbreviations ϕ for $\phi(x,t)$ and ϕ' for $\phi(x,t+1)$ have been used and ∇ is the 2D lattice Laplacian. It should be noted that there is no term *linear* in Δ_t. This is due to the specific form of the decomposition in Eq. (2.9) and the identity

$$\mathrm{Tr}(\{T_iT_j + T_jT_i\}T_k) = 0.$$

The absence of such terms simplifies the calculation since all contributions to the 1D effective action, $S_{\mathrm{eff}}(\Delta)$, are simply given by

$$S_{\mathrm{eff}}(\Delta) = \langle S_I \rangle. \tag{2.14}$$

Other parametrizations require an evaluation of the quadratic terms in $\langle S_I^2 \rangle$. The average is with respect to the fluctuation measure $\exp(S_0)$ taking into account the constraint in Eq. (2.10) which eliminates the zero mode in the x direction. We use the Gaussian results

$$\langle \phi_i \phi_j \rangle = G(0,0)\,\delta_{ij}, \quad \langle \phi_i \phi_j' \rangle = G(0,1)\,\delta_{ij}. \tag{2.15}$$

$G(0,0)$ and $G(0,1)$ are given by the expressions

$$G(0,0) = \int_{-\pi}^{\pi} \frac{dq}{2\pi} \sum_{p=1}^{L-1} \frac{1}{4(\sin^2(\pi p/L) + \sin^2(q/2))}.$$

$$G(0,1) = G(0,0) - \tfrac{1}{4}. \tag{2.16}$$

We use generators defined in Eq. (2.6) with $k=1$ and the identities

$$[T_i, T_j] = -f_{ijk}T_k, \quad f_{ijk}f_{ijl} = \frac{N-2}{2}\,\delta_{kl}, \qquad T_iT_i = \frac{N-1}{4}, \quad \mathrm{Tr}(T_iT_jT_k) = -\tfrac{1}{4}f_{ijk}. \tag{2.17}$$

Then

$$\langle \mathrm{Tr}(\phi^2\Delta^2) \rangle = \langle \mathrm{Tr}(\phi'^2\Delta^2) \rangle = \frac{N-1}{4}\,G(0,0)(-\tfrac{1}{2}\mathbf{\Delta}\cdot\mathbf{\Delta}),$$

$$\langle \mathrm{Tr}(\phi\phi'\Delta^2) \rangle = \frac{N-1}{4}\,G(0,1)(-\tfrac{1}{2}\mathbf{\Delta}\cdot\mathbf{\Delta}),$$

$$\langle \mathrm{Tr}(\phi\Delta\phi'\Delta) \rangle = \frac{N}{4}\,G(0,1)(-\tfrac{1}{2}\mathbf{\Delta}\cdot\mathbf{\Delta}). \tag{2.18}$$

A numerical evaluation of $G(0,0)$ gives

$$G(0,0) = \frac{1}{2\pi}\ln L - A, \quad A = 0.0351637. \tag{2.19}$$

Using Eqs. (2.13)–(2.18), we find

$$S_{\mathrm{eff}}(\Delta) = L\beta_{\mathrm{eff}} \sum_t (-\tfrac{1}{2}\mathbf{\Delta}\cdot\mathbf{\Delta}), \tag{2.20}$$

where

$$\beta_{\mathrm{eff}} = \beta_L - \frac{N-2}{4}\left(\frac{1}{2\pi}\ln L - A\right) - \frac{N}{16}. \tag{2.21}$$

Note that the coefficient of $\ln L$ is b_0 for the coupling $u_L \equiv 1/\beta_L$. Substituting into Eq. (2.8) with $\beta_{\mathrm{QM}} = L\beta_{\mathrm{eff}}$ gives

$$\frac{1}{u(L)} \equiv \frac{1}{m(L)L} = \frac{4\beta_{\mathrm{eff}}}{N-1} = \frac{4}{N-1}\,(\beta_L - b_0(\ln L + \gamma_N)),$$

$$\gamma_N = \frac{\pi N}{2(N-2)} - 2\pi A. \tag{2.22}$$

We thus deduce that

$$\frac{\Lambda_\xi}{\Lambda_L} = \exp(\gamma_N) = \exp\left(-2\pi A + \frac{\pi N}{2(N-2)}\right). \tag{2.23}$$

Using Eq. (2.4) we finally get

$$\frac{\Lambda_{\overline{\mathrm{MS}}}}{\Lambda_\xi} = \sqrt{32}\,\exp(2\pi A), \tag{2.24}$$

which is independent of N.

From Eq. (2.22) we also deduce the tree-level relation

$$u=\frac{N-1}{4}\,u_L\,. \tag{2.25}$$

B. O(N)-spin models

The results for the mass-gap for O(N)-spin models is given to three-loop order in [2] and so we include only a brief outline of the one-loop effective 1D calculation here for completeness. A similar calculation was done by Lüscher [23] but it is instructive to present it in a concise formulation consistent with the previous section. To relate the energy and lattice schemes we use the expansion [10]

$$\langle E\rangle=\frac{N-1}{4\beta_L}\left(1+\frac{1}{8\beta_L}\right)$$

and the definition

$$\beta_E=\frac{N-1}{4\langle E\rangle}$$

to give

$$\frac{\Lambda_E}{\Lambda_L}=\exp\left(\frac{\pi}{4(N-2)}\right).$$

From Ref. [20] we have

$$\frac{\Lambda_{\overline{\rm MS}}}{\Lambda_L}=\sqrt{32}\,\exp\left(\frac{\pi}{2(N-2)}\right).$$

To calculate $m(L)$ on the $L\times T$ strip we use the same method as in the previous subsection with the O(N) spins $s(x,t)$ expressed in terms of the background field Σ_t and the fluctuation field $\phi(x,t)$ as

$$\mathbf{s}(x,t)=\Sigma_t\sqrt{1-\phi(x,t)\cdot\phi(x,t)}+\phi(x,t), \tag{2.26}$$

where $\Sigma_t\cdot\Sigma_t=1$ and $\phi(x,t)$ is an $(N-1)$-dimensional vector satisfying the constraint

$$\sum_x\,\phi(x,t)=0. \tag{2.27}$$

This constraint eliminates the zero-mode divergence in the calculation. We then choose

$$\Sigma_t=\Sigma_0\quad\text{and}\quad\Sigma_{t+1}=e^{\Delta_t T_{12}}\Sigma_0\,, \tag{2.28}$$

where $\Sigma_0=(1,0,0,...,0)$ and Δ_t is the slowly varying 1D background field. T_{12} is the generator of SO(N) rotations in the 1-2 plane. As in the SO(N) case the particular form of the parametrization in Eq. (2.1) ensures that the 1D effective action is given by

$$S_{\rm eff}=\langle S_I\rangle,$$

there being no linear terms in Δ_t in the expansion of the $S(\mathbf{s})$ in Δ and ϕ. The calculation follows the same steps as in the SO(N) case and gives

$$\beta_{\rm eff}=\beta_L-(N-2)\left(\frac{1}{2\pi}\ln L-A\right)-\tfrac{1}{4}, \tag{2.29}$$

where the coefficient of $\ln L$ is identified with b_0 and, as before, $A=0.0351637$. Then

$$\frac{\Lambda_\xi}{\Lambda_L}=\exp\left(-2\pi A+\frac{\pi}{2(N-2)}\right). \tag{2.30}$$

Using $\Lambda_{\overline{\rm MS}}/\Lambda_L$ from above, we conclude that

$$\frac{\Lambda_{\overline{\rm MS}}}{\Lambda_\xi}=\sqrt{32}\,\exp(2\pi A), \tag{2.31}$$

which is identical to the SO(N) result. The two results in Eqs. (2.24) and (2.31) must be the same for $N=3,4$ since the two models have the same continuum limit. That they are independent of N ensures the results are identical for all N. The tree-level relation between couplings is then

$$u=\frac{N-1}{2}\,u_L\,. \tag{2.32}$$

III. SIMULATION AND MEASUREMENT TECHNIQUES

In the following we will give a brief description of our updating algorithm. Similar to Ref. [24] we used an overrelaxation update [25,26] applied to embedded O(2) models. In terms of CPU-time requirements this algorithm outperformed a multigrid algorithm [27] for correlation lengths up to about 20 in the case of the CP^4 model in two dimensions.

In order to save random numbers, and hence CPU time, a large fraction of the Metropolis updates have been replaced by a demon update [28]. Most of the parameters in the algorithm were chosen by trial based on previous experience with the CP^4 model [24].

Our basic update steps are performed on O(2) subgroups of the SO(N) group. We have chosen the same subgroup for each of the sites of the lattice. After a number of sweeps a new subgroup is chosen.

The O(2) subgroups that we consider are given by rotations among two rows or two columns:

$$\begin{aligned}U'_{ki}(x,t)&=s_1(x,t)U_{ki}(x,t)+s_2(x,t)U_{kj}(x,t),\\ U'_{kj}(x,t)&=-s_2(x,t)U_{ki}(x,t)+s_1(x,t)U_{kj}(x,t),\end{aligned} \tag{3.1}$$

with $s_1^2+s_2^2=1$.

This parametrization induces an action for the embedded O(2) model

$$S_{\rm cond}(s)=-\sum_{\langle x,t;x',t'\rangle}\sum_{m,n=1}^{2}c_{mn}(x,t,x',t')s_m(x,t)s_n(x',t'), \tag{3.2}$$

with

$$c_{11}=c_{22}=\beta\sum_k\,U_{ki}(x,t)U_{ki}(x',t')+U_{kj}(x,t)U_{kj}(x',t'),$$

$$c_{12}=-c_{21}=\beta\sum_k\,U_{ki}(x,t)U_{kj}(x',t')-U_{kj}(x,t)U_{ki}(x',t'). \tag{3.3}$$

For the updating of the embedded O(2) model we used a combination of standard Metropolis, demon updates, and microcanonical updates. We apply the microcanonical update step discussed by [26] for the standard XY model in two dimensions. First we compute the sum of the nearest neighbor spins of the site (x,t):

$$R_m = \sum_{(x',t')nn(x,t)} \sum_{n=1}^{2} c_{mn}(x,t,x',t') s_n(x',t'). \quad (3.4)$$

The new values for $\vec{s}$ are then obtained by reflection with respect to $\vec{R}$:

$$\vec{s}' = 2 \frac{\vec{R}\cdot\vec{s}}{\vec{R}^2} \vec{R} - \vec{s}. \quad (3.5)$$

Since $\vec{R}\cdot\vec{s}' = \vec{R}\cdot\vec{s}$ this update step keeps the action constant.

The aim of the demon update is to perform updates similar to a Metropolis update but avoid CPU-intensive parts like the evaluation of trigonometric functions, the exponential function, and pseudorandom numbers.

The demons are introduced by an additional term in the action

$$S' = S + \sum d_{x,t}, \quad (3.6)$$

where the $d_{x,t}$ are positive real numbers. Note that adding the demon part to the action does not change the spin sector of the composite theory. However, the demons give us new options for updates. We start a sequence of demon-updates by a heat-bath step applied to the demons:

$$d = -\ln(\eta), \quad (3.7)$$

where η is a pseudorandom number with a uniform distribution in the interval $]0,1]$. Then we perform updates that keep the composite action of the spin model plus the demons constant, exchanging energy between the demons and the spins. First we compute a proposal for a new spin-value $\vec{s}'$ by reflecting $\vec{s}$ with respect to the sum of the upper and left neighbor spins. Then we check whether the demon at the site can take over the energy without becoming negative. If this is the case, we accept the proposal $\vec{s}'$ and set the demon to its new value. After a sweep of such demon updates we translate the demons on the lattice.

For one given embedding we performed one standard Metropolis sweep, and 10 to 60 overrelaxation sweeps, and finally five demon updates. The number of overrelaxation sweeps was chosen to be roughly proportional to the correlation length.

We alternate the row embedding and the column embedding. The first row (column) is chosen in a fixed sequence from 1 to N, while the second was chosen randomly from the remaining ones.

The improved correlation function estimator

In order to obtain a meaningful result for the step-scaling function the correlation length on the finite lattices has to be computed with an accuracy of less than 1%. In order to achieve this aim we used the improved estimator for the correlation function discussed in Ref. [29] for the case of O(N) vector models.

The underlying physical idea for this improved estimator is similar as that for the one-loop solution of the model discussed in Sec. II. However, here instead of an *effective* one-dimensional model we rather use a *conditional* (or embedded) model. For a given field configuration U the conditional model is defined by

$$S_{\rm cond}(W) = -\beta \sum_t \sum_x \mathrm{Tr}[W(t)U(x,t) \times (W(t+1)U(x,t+1))^T], \quad (3.8)$$

where W is the field of the conditional model. Note that there is no spatial part in the action, since $W(t)$ does not depend on x. Performing the x summation we get

$$S_{\rm cond}(W) = -\sum_t \mathrm{Tr}[Q(t,t+1)W^T(t+1)W(t)], \quad (3.9)$$

where

$$Q(t,t+1) = -\beta \sum_x U(x,t)U^T(x,t+1). \quad (3.10)$$

Reparametrizing the model by $R(t,t+1) = W^T(t)W(t+1)$ we obtain

$$S_{\rm cond}(R) = -\sum_t \mathrm{Tr}[Q(t,t+1)R^T(t,t+1)]. \quad (3.11)$$

For free boundary conditions in time direction there is no constraint on the $R^T(t,t+1)$. Therefore the partition function factorizes, and the solution of the conditional 1D model is reduced to the solution of zero-dimensional systems. The conditional expectation value of the time-slice correlation function is given by

$$\langle G(t,t+\tau)\rangle_{\rm cond} = \mathrm{Tr}[S(t)\langle R(t,t+1)\rangle_{\rm cond} \cdots \langle R(t+\tau-1, t+\tau)\rangle_{\rm cond} S(t+\tau)], \quad (3.12)$$

where

$$S(t) = \sum_x U(x,t). \quad (3.13)$$

We were not able to compute the conditional expectation values exactly. Instead we used Monte Carlo integration for this task. First one has to note that finite statistics for the conditional expectation value does not corrupt the end result for $\langle G(t,t+\tau)\rangle$. Secondly an enormous gain in statistical accuracy can be obtained, since as a consequence of the factorization in Eq. (3.1.5) the statistics of the single ''baby'' Monte Carlo's multiply. Typically we performed 200 Metropolis update steps for the evaluation of $\langle R(t,t+1)\rangle_{\rm cond}$. We used the final value of R for updating the field U. However, we have yet to make careful tests to determine the efficiency gain of this measurement technique.

IV. SIMULATION RESULTS FOR THE SO(4) MODEL

The main object of this investigation was to test the predictions for $m/\Lambda_{\overline{\rm MS}}$ for the SO(N) principal chiral models given by Hollowood [1,19]. The action for the SO(N) matrix models is given in Eq. (1.1). It was found that even for moderate values of N ($N \geq 6$) the continuum limit was difficult to achieve with any degree of confidence, all indications being that a large correlation length is necessary. This is in contrast to recent work on SU(N) models [8,9] where the results indicate that the models are close to the continuum limit even for small ξ ($\xi > 5$). In the next section we will present some results for $N=6$, 8, and 10 to support these statements but will postpone our speculations concerning why such a difficulty occurs until the Conclusion.

In this section we concentrate on the SO(4) model and apply the renormalization scheme described in [2], the ''ξ scheme,'' and compare it with the lattice and energy schemes used in [8,9]. The coupling constant $u(Lm_\infty)$ is defined in Eq. (1.3) [23] and to achieve the continuum limit we require $\overline{u}(Lm_\infty, a/L)$ for fixed Lm_∞ to be essentially independent of a and hence that ξ_∞ is large enough that the a-dependent corrections to Eq. (1.3) are negligible. The problem is that in practice this might require ξ_∞ to be very large indeed and unachievable in a present-day simulation. Alternatively, it might be possible to fit the a dependence in Eq. (1.3) by measuring $\overline{u}(Lm_\infty, a/L)$ for various ξ_∞ with Lm_∞ fixed, and extrapolating to $a/L=0$. In the case that the corrections are perturbative they behave as $O(a^2)$. Whether or not this is the case must be deduced from the simulation and for the SO(4) model there is clear evidence that a simple perturbative interpretation of the a-dependent effects is not possible for the values of ξ_∞ we use. Nevertheless we try to extrapolate the results to the continuum limit in a reliable way and compute the value of $\overline{u}(2, a/L)$. It must be emphasized that it is crucial to determine this value of u as accurately as possible since it is the starting point for the subsequent determination of u at smaller scales, and ultimately contributes to the systematic error on the computation of $m/\Lambda_{\overline{\rm MS}}$. In order to

TABLE I. The values of $\overline{u}(2, a/L)$ in lattice and energy methods as a function of ξ_∞. The energy method shows plausible convergence to the extrapolated value $u(2)=2.25(2)$.

β_L	$\langle E \rangle$	ξ_∞	$\overline{u}(2,a/L)$ Lattice method	$\overline{u}(2,a/L)$ Energy method
1.05	0.5411(2)	3.71(3)	1.98(1)	2.44(1)
1.10	0.4702(2)	8.34(7)	2.07(1)	2.35(2)
1.12	0.4435(1)	13.62(13)	2.11(1)	2.27(2)
1.14	0.42176(6)	25.3(4)	2.17(2)	2.26(2)

TABLE II. Couplings measured in the lattice and energy methods for different values of L/a. The a-dependent violations to finite-size scaling are most pronounced for $Lm_\infty \sim 1$. The energy method was not used where it gave little information in addition to the lattice method. The statistical errors of $\tilde{u}(2L/a)$ which are not quoted here are of similar size as those of $\tilde{u}(L/a)$ coupling values.

				$\Sigma(1/2, \tilde{u}(2L/a)) \equiv \tilde{u}(L/a)$	
L/a	β_L	$\langle E \rangle$	$\tilde{u}(2L/a)$	Lattice method	Energy method
8	1.0908	0.4531(5)	2.25	1.590(10)	1.727(10)
14	1.1169	0.4352(3)	2.25	1.647(8)	1.720(8)
26	1.1393	0.4186(2)	2.25	1.711(7)	1.737(7)
40	1.15335	0.40915(7)	2.25	1.734(7)	1.747(7)
7	1.1088	0.4347(3)	1.747	1.416(3)	1.475(3)
13	1.1347	0.4194(2)	1.747	1.469(3)	1.480(3)
20	1.15235	0.4082(1)	1.747	1.492(3)	1.499(3)
30	1.16917	0.39778(6)	1.747	1.506(3)	1.509(3)
10	1.1484	0.4111(1)	1.517	1.323(2)	
15	1.1659	0.3989(1)	1.517	1.340(3)	
20	1.1803	0.3911(1)	1.517	1.345(2)	
5	1.1424	0.4074(3)	1.351	1.203(2)	
10	1.1789	0.3906(2)	1.351	1.212(2)	
16	1.2045	0.3784(1)	1.351	1.218(2)	
8	1.2028	0.3774(2)	1.222	1.113(1)	
16	1.245	0.36014(9)	1.222	1.114(1)	
8	1.2452	0.3587(2)	1.115	1.025(1)	
16	1.2914	0.34215(8)	1.115	1.024(1)	
8	1.2922	0.3408(2)	1.0234	0.9494(7)	
16	1.3368	0.32681(7)	1.0234	0.954(1)	
8	1.3357	0.3264(1)	0.948	0.8902(5)	
16	1.3851	0.31230(6)	0.948	0.8910(4)	
8	1.3849	0.3116(1)	0.891	0.8355(5)	
16	1.4356	0.29861(6)	0.891	0.8342(5)	

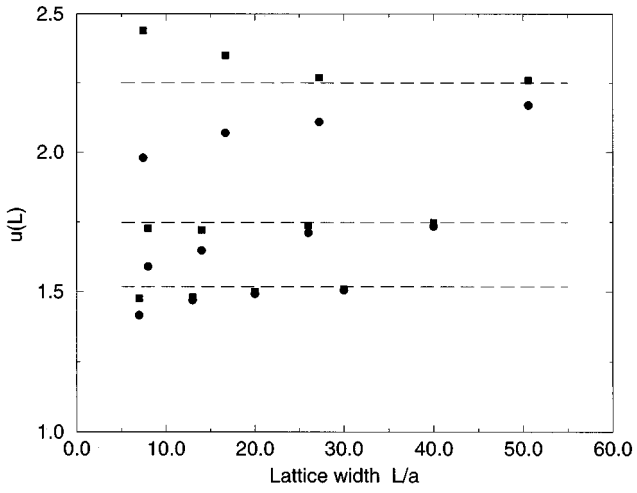

FIG. 1. Values of the coupling $\overline{u}(Lm_\infty, a/L)$ from Tables I and II plotted against L/a for Lm_∞ fixed at the values 2,1,1/2. The violations of the finite-size scaling assumption are clearly evident for both versions of the ξ scheme used: the lattice scheme (●) and the energy scheme (■). In each case the value assumed for the extrapolation to $a=0$ is shown as the dashed line.

attain the continuum limit we measured $u(2)$ for increasing values of ξ_∞ and fitted the a dependence and so deduced the continuum coupling, $u(2)$. We characterized the theory either by the lattice coupling β_L or by the coupling defined by Parisi [18] in terms of the internal energy, Eq. (2.1):

$$\beta_E = \frac{N-1}{8\langle E\rangle}. \tag{4.1}$$

Note $\langle E\rangle$ is normalized to lie in [0,1]. We found that $\langle E\rangle$ suffered from strong finite-size effects and so could not be expressed as a function of β_L alone. We chose to measure $\overline{u}(Lm_\infty, a/L)$ by keeping either β_L or β_E constant on the lattices with $L/a \gg \xi_\infty$ and $L/a = 2\xi_\infty$, denoted the ''lattice'' and ''energy method,'' respectively. Because of the finite-size effects observed in $\langle E\rangle$ this will lead to different estimates for $\overline{u}(2, a/L)$ and by trial we can see which method gives the better extrapolation to $a/L=0$. Where $L/a = 2\xi_\infty$ was nonintegral, simulations were done for the integer L/a values either side of $2\xi_\infty$ and interpolation used to deduce $\xi(L)$. The results are shown in Table I where we can see that the energy method shows better convergence than the lattice method. The errors shown are statistical and a naive straightforward extrapolation gives the value $u(2)=2.25(2)$ for the continuum coupling constant. However, we shall argue below that while plausible this value for $u(2)$ is incorrect since the convergence to the continuum is only apparent not real.

That $\langle E\rangle$ is sensitive to the lattice size is another indication that SO(N) models are more complex in the continuum limit than SU(N) models where no such effect is observed. We find that the finite-size effects in $\langle E\rangle$ largely seem to offset those in $\overline{u}$ which indicates that there is some connection between the short- and long-range properties of the system. From Table I it can also be seen that the a-dependent effects in the lattice method are not fitted by a perturbative parametrization: they are closer to a $a^{1/2}$ dependence. This indicates that nonperturbative contributions are strong and that their effect on the calculation of $u(2)$ seems to be largely accounted for using the energy method. These are all reasons why we should be cautious and suspicious of assuming that we are observing properties of the continuum theory.

One reasonable test that we are simulating the continuum theory is to check that the computed value of $m/\Lambda_{\overline{\rm MS}}$ agrees with the theoretical prediction. We thus compute the step-scaling function described in [2] and Sec. I and fit the short-distance behavior of u to the form deduced from perturbation theory. We choose the factor for the scale change to be $s=1/2$. Therefore we consider pairs of lattices with sizes $2L$ and L, respectively, and β_L is adjusted so that $\tilde{u}(2L/a, \beta_L)$ is a required value. Then $\tilde{u}(L/a, \beta_L)$ is measured in both the lattice and energy schemes, that is, keeping either β_L or β_E constant on the lattice pair. Various values of L/a were chosen so that the a-dependent effects can be determined and eliminated by extrapolation. When we believe that the continuum limit has been attained than the step scaling function

TABLE III. The sequence of continuum couplings as a function of Lm_∞. Also shown are the one- and two-loop approximations to $\sigma(1/2,u)$ evaluated with $u=u(2Lm_\infty)$. These should be compared with the Monte Carlo result $\sigma(1/2,u(2Lm_\infty))_{\rm MC}=u(Lm_\infty)$. It seems plausible that asymptotic scaling sets in for $Lm_\infty \geqslant 1/4$.

			$\sigma(1/2,u(2Lm_\infty))$		
Lm_∞	$u(2Lm_\infty)$	$u(Lm_\infty)$	One loop	Two loop	Three loop
1	2.25	1.754(13)	1.9305	1.9010	1.8915
0.987/2	1.747	1.517(6)	1.5481	1.5329	1.5291
0.987/4	1.517	1.351(6)	1.3647	1.3544	1.3521
0.987/8	1.351	1.222(4)	1.2289	1.2214	1.2199
0.987/16	1.222	1.1148(21)	1.1212	1.1154	1.1145
0.987/32	1.1148	1.0234(15)	1.0303	1.0259	1.0252
0.987/64	1.0234	0.9478(11)	0.9518	0.9483	0.9478
1.073/128	0.9561	0.8912(12)	0.8933	0.8904	0.8900
1.073/256	0.8912	0.8339(12)	0.8364	0.8340	0.8337

TABLE IV. Computed values for $m/\Lambda_{\overline{\rm MS}}$ using the two- and three-loop β function for the coupling evaluated at the indicated scale (the small adjustments to the scale explicit in Table III are omitted for clarity). The errors are calculated from the accumulation of statistical errors at all preceding steps.

Lm_∞	1/256	1/128	1/64	1/32	1/16	1/8	1/4	1/2	1/1
$m/\Lambda_{\overline{\rm MS}}$ Two loop	14.3(1.0)	14.3(1.0)	14.4(9)	14.4(9)	14.1(9)	14.1(9)	14.2(9)	14.0(7)	13.2(5)
$m/\Lambda_{\overline{\rm MS}}$ Three loop	13.7(1.0)	13.6(1.0)	13.7(9)	13.6(9)	13.3(9)	13.2(9)	13.2(9)	12.9(7)	12.0(5)

σ can be determined from Eq. (1.5) and compared with perturbation theory using Eqs. (1.6) and (1.7):

$$b_0=\frac{N-2}{2\pi(N-1)},\quad b_1=\frac{b_0^2}{2}.$$

The first two coefficients of the β function quoted for u are obtained from those associated with $u_L=1/\beta_L$ [20] by using Eq. (2.25) gives the tree-level relation

$$u=\frac{N-1}{4}\,u_L\,.$$

The results are shown in Table II.

In each case the continuum coupling for a given scale was determined by extrapolation to $a=0$. From Table II it can be seen that the most care needs to be taken when $Lm_\infty\sim 1$ where the corrections to finite-size scaling are the greatest. In all cases the energy method was the most convergent, but for sufficiently large L both the lattice and energy methods were compatible and a common value for the continuum coupling was consistent (see Fig. 1). For $Lm_\infty<1/2$ the a-dependent corrections were small and consistent with perturbation theory and both schemes gave consistent results. Following Eq. (1.8) we tried to use the result of a given step as the argument of the next step. This was achieved in all cases except when $Lm_\infty=1/2$ and $Lm_\infty=1/128$ where we corrected the small mismatches by interpolation. These corrections lead to scale changes of 2.026 and 1.840, respectively. The sequence of continuum couplings deduced are shown in Table III.

Also shown are the one-, two-, and three-loop approximations to $\sigma(1/2,u)$ evaluated with $u=u(2Lm_\infty)$. These should be compared with the Monte Carlo result

$$\sigma(1/2,u(2Lm_\infty))_{\rm MC}=u(Lm_\infty).$$

TABLE V. The values of $m/\Lambda_{\overline{\rm MS}}$ in the lattice and energy schemes [12, 10, 8, 9] as a function of ξ_∞ for the SO(4) model. The theoretical prediction is $m/\Lambda_{\overline{\rm MS}}=3.87153$ [1,19].

			$m/\Lambda_{\overline{\rm MS}}$	
β_L	$\langle E\rangle$	ξ_∞	Lattice scheme	Energy scheme
1.05	0.5411(2)	3.71(3)	305(2)	20.4(2)
1.10	0.4702(2)	8.34(7)	248(2)	31.3(3)
1.12	0.4435(1)	13.62(13)	194(2)	34.1(3)
1.14	0.42176(6)	25.3(4)	133(2)	30.9(5)
1.15	0.41291(5)	33.4(8)	114(3)	29.5(7)

Clearly asymptotic scaling sets in for $Lm_\infty\leqslant 1/4$. It is perhaps surprising that the two-loop approximation fits the Monte Carlo results so well at such relatively large scales, but it gives confidence that we can probe deeply into the region where asymptotic scaling holds and hence that perturbative parametrization of u in terms of $\Lambda_{\overline{\rm MS}}$ is valid. The a dependence of the results for these smaller values of u indicates that β_L is large enough for the extrapolation to the continuum limit, $a=0$, to be reliable. The data from Table III are shown in Fig. 2 where the computed function $\sigma(2,u)$ is compared with its one- and three-loop approximations deduced from Eqs. (1.6) and (1.7). The important intermediate region where it is crucial to maintain the continuum limit in order to reliably relate the low and high energy scales is also in clear evidence. This match between the small-L region and large-L region [where trivially $u(Lm_\infty)=Lm_\infty$] is the important part of the simulation.

From Table III we can deduce the value of m/Λ_ξ, i.e., in the ξ scheme, using the two-loop formula, Eq. (1.9). We have

$$\Lambda_\xi^{(2)}=\frac{1}{L}\left(\frac{u}{3\pi}\right)^{-1/2}\exp\left(-\frac{3\pi}{u}\right).\tag{4.2}$$

In fact, since the covering group of SO(4) is SU(2)⊗SU(2) and the SU(2) matrix model is isomorphic to the O(4) spin model, we are able to use the three-loop β function in Ref. [2] to deduce that

$$\Lambda_\xi^{(3)}=\Lambda_\xi^{(2)}\left(1-\frac{1}{6\pi}\,u\right).\tag{4.3}$$

A discussion of the detailed relationship between these models will be postponed until the next section but it is convenient to invoke this formula here. The one-loop calculation necessary to determine the ratio $\Lambda_\xi/\Lambda_{\overline{\rm MS}}$ is given in Sec. II, and using the result for Λ_L/Λ_ξ and $\Lambda_{\overline{\rm MS}}/\Lambda_L$ from Eqs.

TABLE VI. The values of $\overline{u}(1,1/\xi_\infty)$ in the lattice method as a function of ξ_∞. Interpolation is used to calculate $\overline{u}$ at noninteger values of L. Clearly, finite-size scaling violations are small and, within the errors, not incompatible with the perturbative prediction that they behave like $O(a^2)$.

β_L	$\langle E\rangle$	χ	ξ_∞	$\overline{u}(1,1/\xi_\infty)$
2.00	0.4230(2)	99.8(3)	7.89(2)	1.552(5)
2.20	0.3775(1)	266.6(8)	13.95(5)	1.562(4)
2.40	0.34070(5)	555.7(1.9)	25.7(1)	1.585(5)
2.60	0.31071(2)	1629.9(2.6)	47.07(8)	1.584(3)

(2.14) and (2.23), we give the computed two- and three-loop results for $m/\Lambda_{\overline{\rm MS}}$ versus length scale in Table IV. The prediction for this quantity can be taken from the paper by Hollowood [1] where the formula for $m/\Lambda_{\overline{\rm MS}}$ for the SO(N) matrix models can be extended down to $N=4$ [19]. The prediction is

$$\frac{m}{\Lambda_{\overline{\rm MS}}}=\frac{2^{7/2}}{\sqrt{\pi e}}=3.8715. \tag{4.4}$$

As can be seen from Table IV the computer results are wrong by a minimum of a factor of 4. The inescapable conclusion is that we have not eliminated corrections to finite-size scaling and are not close to the continuum limit in our simulation. Without the theoretical prediction we might have been persuaded that the evidence did point to the simulation having produced reliable continuum results—the step scaling function seemed to agree well with the two-loop prediction already by scales $Lm_\infty \leqslant 1/4$ and from Table IV the results seem stable across a wide range of length scales. This is deceptive since the crucial part of the simulation where the finite-size scaling assumption is most strongly violated is for lattices where $Lm_\infty \sim 1$ and the parts of the simulation which are important for setting the scale are not probing the continuum. The corollary is that we need the initial value of $\xi_\infty = 1/am_\infty$ to be considerably larger than the biggest we have taken. The surmise is that since the SO(N) manifold is not simply connected, $\Pi_1[{\rm SO}(N)]=Z_2$, there are vortices which are responsible for nonperturbative violations of finite-size scaling and much larger values of β are needed before their effect is sufficiently suppressed so that the continuum limit can be approached in a controlled, perturbative, way. One check is therefore to simulate the covering group of SO(4), SU(2)⊗SU(2), and see whether the problems with finite-size scaling violations are perturbative. The results are presented in the next section.

We can also check what happens if we apply the method used in Refs. [12,10,8,9] for the couplings defined in Eq. (1.11). These bare couplings are defined to be evaluated at the scale of the lattice spacing a. The Λ parameters of the respective lattice and energy schemes, Λ_L and Λ_E, can be calculated using Eq. (1.9). Since the corresponding value of am_∞ is known from the simulation the estimate for $m/\Lambda_{\overline{\rm MS}}$ can be calculated using Eqs. (2.3) and (2.4). The results are shown in Table V. The results are very poor and it is clear that the approach is hopeless. This should be contrasted with the success of the method applied to SU(N) matrix models [8,9] and the O(4) and O(8) spin models [10].

V. RESULTS FOR THE SU(2)⊗SU(2) COVERING OF SO(4)

The SU(2)⊗SU(2) matrix model consists of two independent SU(2) models and the SU(2) matrix model is isomorphic to the O(4) spin model where the fields take values in O(4)/O(3)≡S^3. Thus we need only to simulate the O(4) spin model which can be done using the cluster algorithm [11]. The theoretical prediction for $m/\Lambda_{\overline{\rm MS}}$ is given in [7,6] to be

$$m/\Lambda_{\overline{\rm MS}}=\sqrt{\frac{32}{\pi e}}=1.9358. \tag{5.1}$$

The only difference between the SO(4) and SU(2) matrix models is that the lightest state of the SU(2) model is a spinor and that of the SO(4) model corresponds to a spinor-antispinor state which is not, in fact, bound. Thus, in the SO(4) model, the large time asymptotics of the correlator are controlled by the spinor-antispinor cut and not a bound state pole. However, in two dimensions the large time behavior is dominated by the branch point mass with only slow power-law deviations from a pure exponential decay. Thus we simply have

$$m_{\rm SO(4)}=2m_{\rm SU(2)}. \tag{5.2}$$

This factor of 2 simply converts the SO(4) prediction of Hollowood [1] into the prediction of Hasenfratz *et al.* [7,6] for the O(4) spin model. It then follows that the two continuum couplings defined as in Eq. (1.3) are related by a factor of 2:

$$u_{\rm SO(4)}=2u_{\rm SU(2)}. \tag{5.3}$$

We shall omit the distinguishing subscript on u unless it is necessary to avoid ambiguity.

The action for the O(4) spin model is taken to be

$$S(\mathbf{s})=\beta_L\sum_{n,\mu}\mathbf{s}_n\cdot\mathbf{s}_{n+\mu}. \tag{5.4}$$

As before we define u using Eqs. (1.2) and (1.3). The tree-level result from Sec. II B relating the ξ and lattice schemes is

TABLE VII. Couplings measured in the lattice method for different values of L/a. The a-dependent violations of finite-size scaling are apparent but small, even for the crucial case where $L/a\sim\xi_\infty$.

L/a	β_L	$\langle E\rangle$	χ	$\tilde{u}(2L/a)$	$\Sigma(1/2,\tilde{u}(2L/a))\equiv\tilde{u}(L/a)$
4	1.9874	0.4037(3)	18.25(3)	1.584(5)	1.208(3)
7	2.1914	0.3714(2)	47.87(6)	1.584(4)	1.210(3)
13	2.4032	0.3378(1)	140.8(2)	1.584(3)	1.219(2)
24	2.6050	0.30941(3)	415.3(4)	1.584(3)	1.227(1)
8	2.4649	0.3264(1)	78.0(1)	1.228(3)	1.008(2)
16	2.6959	0.29735(5)	268.0(3)	1.228(2)	1.011(2)
8	2.6954	0.29579(7)	96.5(1)	1.011(2)	0.865(1)
16	2.9260	0.27185(4)	337.9(4)	1.011(2)	0.863(1)

TABLE VIII. The sequence of continuum couplings for the O(4) spin model as a function of Lm_∞. Also shown are the one-, two-, and three-loop approximations to $\sigma(1/2,u)$ evaluated with $u=u(2Lm_\infty)$. These should be compared with the Monte Carlo result $\sigma(1/2,u(2Lm_\infty))_{\rm MC}=u(Lm_\infty)$. Clearly, asymptotic scaling is already setting in for $Lm_\infty \leqslant 1$.

			$\sigma(1/2,u(2Lm_\infty))$		
Lm_∞	$u(2Lm_\infty)$	$u(Lm_\infty)$	One loop	Two loop	Three loop
2/1	4.132(10)	2.309(10)	2.5700	2.2927	2.1062
1/1	2.309(10)	1.584(4)	1.7236	1.6384	1.5925
1/2	1.584(4)	1.228(3)	1.2847	1.2495	1.2348
1/4	1.228(2)	1.011(3)	1.0401	1.0216	1.0152
1/8	1.011(2)	0.863(2)	0.8801	0.8689	0.8657

$$u=\frac{N-1}{2}\,u_L\,. \tag{5.5}$$

Using this result, the β function for u as defined in Eq. (1.7) then has coefficients

$$b_0=\frac{N-2}{\pi(N-1)},\quad b_1=\frac{N-2}{\pi^2(N-1)^2},\quad b_2=\frac{N-2}{\pi^3(N-1)^2}. \tag{5.6}$$

The result for b_2 is taken from Ref. [2]. In addition to the two-loop formula for Λ_ξ, Eq. (1.9), we have the three-loop formula

$$\Lambda_\xi^{(3)}=\Lambda_\xi^{(2)}\left(1-\frac{1}{\pi(N-1)}\,u\right). \tag{5.7}$$

Because the continuum limits of the SO(4) and O(4) spin model are controlled by the same Lie algebra the conversion ratio $\Lambda_\xi/\Lambda_{\overline{\rm MS}}$ is the same for both. However, as a check and for completeness, the one-loop calculation which yields this conversion ratio for the general O(N) spin model is briefly described in Sec. II B. Of course, for $N=4$ all necessary results can be taken from Ref. [2] .

The simulation results for $u(1)$ for various values for ξ_∞ are shown in Tables VI and VII and the results for the corresponding step-scaling function are given in Table VIII where the values quoted have been extrapolated to the $a=0$ limit. Clearly the violations of finite-size scaling are much smaller than for the SO(N) matrix model, compare with Tables I and II, and are compatible, within errors, with the perturbative prediction that they behave like O(a^2). In comparing Tables VII and II the conversion factor of two between couplings, Eq. (5.3), should be borne in mind. Note that we have not used the energy method for the spin model since it is not needed.

The two-loop and three-loop computed values of $m/\Lambda_{\overline{\rm MS}}$ are given in Table IX. The two loop result is already near to the predicted value of 1.9385 for $Lm_\infty \sim 1/8$ and the three-loop result agrees with this prediction within errors even for $Lm_\infty \sim 1$. In Fig. 2 we compare the SU(2)$\otimes$SU(2) and SO(4) results for the step-scaling function. We have plotted $u_{\rm SO(4)}$ and $2u_{\rm SU(2)}$ on the ordinate since in the continuum limit the data points should coincide up to the small correction factors

TABLE IX. Computed values for $m/\Lambda_{\overline{\rm MS}}$ using the two-loop and three-loop β functions for the coupling evaluated at the indicated scale. The errors are calculated from the accumulation of statistical errors at all preceding steps. These results are to be compared with the theoretical prediction [7,6] $m/\Lambda_{\overline{\rm MS}}=1.9358$.

$L/a\xi_\infty$	1/8	1/4	1/2	1/1
$m/\Lambda_{\overline{\rm MS}}$ Two loop	1.783(30)	1.735(28)	1.679(18)	1.609(10)
$m/\Lambda_{\overline{\rm MS}}$ Three loop	1.963(33)	1.944(31)	1.930(20)	1.935(11)

of Table III. Also shown are the curves for $\sigma(1/2,u)$ derived from the one-loop and three-loop β functions. The large u result, $\sigma(1/2,u)\to u/2$, to which all curves should eventually be asymptotic is also shown. It can be seen that there is a clear deviation between the results for the two models in the crucial region where $Lm_\infty \sim 1$, but that the SO(4) result lies close to the perturbative prediction, tempting us to conclude that the SO(4) simulation is sufficiently close to the continuum limit. This is wrong.

The calculations of $m/\Lambda_{\overline{\rm MS}}$ in the lattice and energy schemes have been done using three-loop results by Wolff in Ref. [10]. Our simulation results agree in detail with his and he finds general agreement with the prediction for $m/\Lambda_{\overline{\rm MS}}$. However, the different schemes tried by Wolff do show different rates of convergence to theory as a function of ξ_∞ the best being the energy scheme which agrees very well with theory for $\xi_\infty \sim 10$. We have similarly good agreement for the ξ scheme confirming the ease with which the continuum limit can be controlled.

VI. RESULTS FOR SO(N), $N=6,\ 8,\ 10$

We attempted to analyze the SO(N) models for $N=6,\ 8,\ 10$ in the same way as for SO(4). However, the

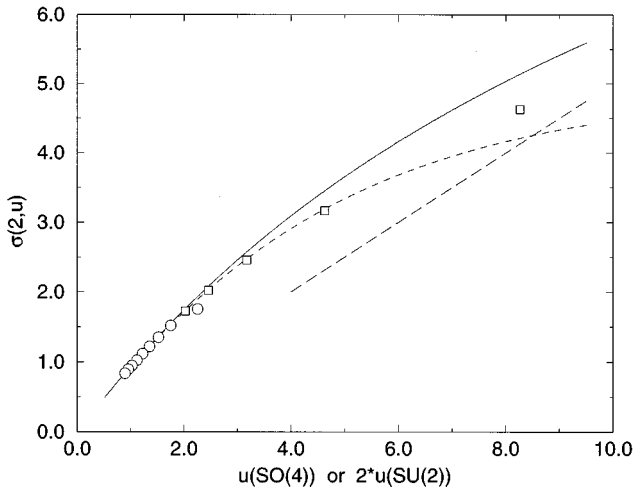

FIG. 2. The step-scaling function $\sigma(1/2,u)$ versus u. The solid and dashed curves are respectively the one- and three-loop perturbative calculations. Data for the SO(4) matrix model (○) and the SU(2)$\otimes$SU(2) matrix model (□). The large u result to which all curves are asymptotic is shown as the long-dashed line.

TABLE X. The values of $m/\Lambda_{\overline{\rm MS}}$ computed in the lattice and energy schemes compared with the theoretical prediction for $N=6$, 8, 10. There is no agreement between the schemes and no trend suggesting that the results will converge to the prediction.

				$m/\Lambda_{\overline{\rm MS}}$		
N	β_L	$\langle E\rangle$	ξ_∞	Lattice scheme	Energy scheme	Theory
6	1.5	0.6786(1)	1.387(3)	48.8(1)	5.32(1)	3.87153
6	1.6	0.6226(1)	1.97(1)	62.3(3)	6.03(3)	3.87153
6	1.7	0.5181(3)	4.85(4)	46.0(4)	7.98(7)	3.87153
6	1.73	0.4784(2)	8.7(1)	30.7(3)	8.07(9)	3.87153
8	2.28	0.5727(3)	2.80(2)	35.3(3)	5.27(4)	3.65837
8	2.31	0.5362(4)	3.98(3)	28.0(2)	5.55(4)	3.65837
8	2.33	0.5073(3)	5.75(7)	21.0(3)	5.51(7)	3.65837
8	2.35	0.4851(2)	8.05(6)	16.2(1)	5.36(4)	3.65837
10	2.91	0.5623(2)	3.05(1)	25.13(8)	4.65(2)	3.523789
10	2.93	0.5341(4)	4.18(3)	19.46(14)	4.61(3)	3.523789
10	2.95	0.5054(2)	5.90(3)	14.63(7)	4.62(2)	3.523789

CPU time required is prohibitively large and we were unable to work with sufficiently large correlation lengths. It is instructive, however, to compute the values of $m/\Lambda_{\overline{\rm MS}}$ for each model in the lattice and energy schemes. The results are shown in Table X. While the energy scheme does not show the large deviation from theory of the SO(4) model the results are clearly untrustworthy. There is no agreement between the different schemes and, although the range of ξ used was limited, there is no indication that the results are converging towards the correct answer. The contrary is true for SU(N) [8,9] where the agreement with theory was good even for the modest values of ξ similar to those used in this present study. It is interesting to note that for $N=8$, 10 the energy scheme gives results which seem independent of ξ_∞ for the restricted range covered. Clearly, this cannot be taken as indicating that the results have converged to the $\xi_\infty\to\infty$ limit: in light of our experience it shows very little.

Another prediction derived from the exact S matrix is for the mass ratios of particles in the theory. For SO(N)(N even) the prediction is

$$\frac{m_p}{m}=\frac{\sin[\pi p/(N-2)]}{\sin[\pi/(N-2)]}, \quad 1<p\leqslant(N-2)/2, \tag{6.1}$$

where p labels the pth species and m is the mass of the lightest state. We simulated the SO(N) model for $N=6$, 8, 10 and measured the masses in the different channels labeled by p. Hollowood [1] has discussed the relevant interpolating operators for these states and we choose the simplest operators which couple to the desired state in each channel. The operator for the pth state is

$$O_p(x)_{i_1\cdots i_p j_1\cdots j_p}=\sum_{\text{perms of } j_1\cdots j_p}(-1)^P U(\mathbf{x})_{i_1 j_1}\cdots U(\mathbf{x})_{i_p j_p}, \tag{6.2}$$

where P is the permutation signature of the ordering of the $\{j_i\}$. Thus O_p is the outer product of p matrices antisymmetrized on the row and column labels, respectively. The corresponding Green function is

$$G_p(x)=\langle \mathrm{Tr}(O_p(\mathbf{x})O_p^T(0))\rangle_c, \tag{6.3}$$

where the trace has the obvious meaning. The results for the mass ratios m_2/m for $N=8$, 10 and m_3/m for $N=10$ are shown in Table XI.

There is no convincing agreement between simulation and theory and, moreover, no trend suggesting that the discrepancy is $\sim a^2$.

VII. DISCUSSION

The main result of this paper is that the properties of the continuum SO(4) theory cannot be observed in a simulation of the lattice-regularized model for the values of β_L and correlation lengths accessible to current computers. We have shown that no such difficulty occurs for the model based on the SU(2)⊗SU(2) cover of SO(4). We believe that both models give rise to the same continuum theory, characterized by the fixed point at $\beta_L=\infty$, but that the ways in which this continuum theory is approached in the lattice-regularized versions are very different. For SU(2)⊗SU(2) finite-size scaling with O(a^2) deviations holds for the range of couplings used, and for scales $Lm_\infty<1$ the flow with L of the renormalized coupling, $u(Lm_\infty)$, is well given by the three-loop β function. The value for $m/\Lambda_{\overline{\rm MS}}$ computed in the simulation agrees well with the theoretical prediction (Table IX). In contrast, for SO(4) the violations of scaling do not fit an O(a^2) form but do seem to diminish to zero (see Fig. 1) as ξ_∞ increases. This apparent or ''pseudoscaling'' can be wrongly interpreted as signalling the continuum theory and can deceive us into believing that the value for the continuum coupling can be deduced. The false nature of this pseudoscaling is exposed by comparing the resulting computed value for $m/\Lambda_{\overline{\rm MS}}$ of ~14 with the theoretical prediction of 3.8715. We also find no convergence to a result for $m/\Lambda_{\overline{\rm MS}}$ using the lattice and energy schemes for SO(4). In contrast for SU(2)⊗SU(2) the lattice scheme gives an acceptable result although clearly inferior to that of the ξ scheme.

We analyzed data for the SO(N) models with $N=6$, 8, 10 and used the lattice and energy schemes to attempt to obtain an estimate for $m/\Lambda_{\overline{\rm MS}}$. The results are shown in Table X

TABLE XI. The computed mass ratios for $N=8$, 10 compared with the predictions. There is no convincing agreement between simulation and theory.

			m_2/m		m_3/m	
N	β_L	ξ_∞	Simulation	Theory	Simulation	Theory
8	2.28	2.80(2)	1.84(1)	1.732		
8	2.31	3.98(3)	1.79(3)	1.732		
8	2.33	5.75(7)	1.83(2)	1.732		
8	2.35	8.05(6)	1.85(2)	1.732		
10	2.91	3.05(1)	1.89(2)	1.848	2.7(2)	2.414
10	2.93	4.18(3)	1.93(2)	1.848	2.73(3)	2.414
10	2.95	5.90(3)	1.91(2)	1.848	2.73(3)	2.414

and it is clear that there is no agreement between the schemes nor with the theoretical prediction. We also computed the mass ratios of the fundamental masses predicted by Ogievetsky *et al.* [5] and the results are given in Table XI. There is a persistent discrepancy up to 10% and there is no sign of a trend to the correct values as β_L increases. These results support the conjecture that we are unable to simulate the continuum theory for SO(N) models with present computer resources.

The discrepancy between the computed and theoretical values of $m/\Lambda_{\overline{\rm MS}}$ is much larger than that of about 10% reported by Lüscher *et al.* in their analysis of the O(3) spin model [2], which they attributed to the truncation of the perturbative β function at three-loop order. This is not the resolution of the problem we have found for the SO(4) model. We conjecture that the difference lies in the different connectivities of the underlying manifolds: the SO(N) models contain Z_2 vortex lattice artifacts while the covering group models do not. In the general SO(N) case the cover is Spin(N) which is constructed from the associated Clifford algebra [30]. The vortices create an obstruction to observing the fixed point at $\beta_L=\infty$ but are eventually suppressed at sufficiently large β_L. Recent work by Hasenbusch [16] and Niedermayer *et al.* [17] has discussed a similar phenomenon comparing the O(3) and RP^2 spin models. They propose a similar conclusion, namely that the difference between the two models is due to lattice vortex artifacts and the onset of scaling in the RP^2 model is delayed but that for restricted ranges of the coupling the violations of scaling vary only slowly giving rise to the misinterpretation that true scaling has set in. From Fig. 1 we might confidently deduce that $u(2)=2.25$ but from our simulation of the covering group we find that the value should be $u=3.17$. We expect that as β_L increases a crossover phenomenon will occur where the violations to scaling will again become large and then eventually diminish to become $O(a^2)$ allowing the true scaling limit to appear. It is important to estimate the value of β_L and ξ_∞ above which finite-size scaling and the continuum theory limit should be observed. A crude attempt can be made with current data by using the theoretical prediction for $m/\Lambda_{\overline{\rm MS}}$ together with

$$\xi_\infty=\frac{L/a}{m/\Lambda_\xi}(b_0u(Lm_\infty))^{1/2}\exp\left(\frac{1}{b_0u(Lm_\infty)}\right), \quad (7.1)$$

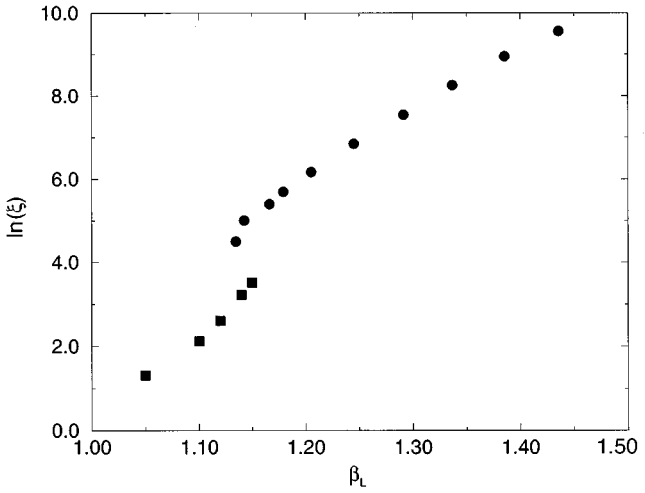

FIG. 3. $\ln(\xi_\infty)$ plotted versus β_L derived from the short-distance behavior and the two-loop β function (●) and from direct measurement in the simulation (■). The two sets of results do not agree indicating that the large scale properties are not controlled by the continuum theory.

to deduce $\xi_\infty(\beta_L)$ from the data for $u(Lm_\infty)$ at sufficiently small Lm_∞ given in Table III. These results for $\xi_\infty(\beta_L)$ can be compared with the results for $\xi_\infty(\beta_L)$ computed directly from simulation. If the lattice theory is near the continuum limit these alternative methods of computing $\xi_\infty(\beta_L)$ should give similar answers. There is consistency to within 10% for the values $\xi_\infty(\beta_L)$ from using similar values of β_L on lattices of different widths corresponding to different measured values of $\tilde{u}$. Where there is a choice we have taken the result from the smallest $\tilde{u}$. We plot $\ln(\xi_\infty)$ versus β_L in Fig. 3 for both approaches. The mismatch is clear for $\beta_L\sim1.15$: the direct measurement gives $\xi_\infty=33.4(8)$ whereas the short-distance result is $\xi_\infty\sim150$. It seems reasonable to infer that the two methods will not agree until $\xi_\infty\gg150$.

The perturbative step-scaling function is well reproduced for sufficiently small scales even though the observables on scales $Lm_\infty\sim1$ show a large departure from continuum behavior. In this context note that $\sigma(1/2,u)$ for $u=2.25$ is actually quite close to the three-loop prediction even though the true scale associated with this value is a factor of about 4 different from that assigned in the simulation. Thus near agreement with the perturbative prediction at small scales is not sufficient to infer that the continuum theory is being observed at large scales: from our simulation of the covering group the correct value for u at the scale assigned in this case is $u=3.17$ and $\sigma(1/2,u)$ for this value agrees very well indeed with the three-loop perturbative prediction (see Fig. 2).

Suppose we were able to simulate at, say $\beta_L\sim1.18$ on a large enough lattice. From our results we see that the properties of the continuum theory are well reproduced at scales $Lm_\infty<1/8$ but from the above discussion we would expect the direct measurement of ξ_∞ to be considerably less than the short-distance prediction of $\xi_\infty\sim300$. So while the properties of the continuum theory are computable at short distances for $\beta_L\sim1.18$ the long distance results do not reflect the continuum but are dominated by residual lattice artifacts: vortices in the SO(4) model.

For a Euclidian continuum field theory a field configuration can be viewed as a map of the space R^2 onto the manifold of the field. A vortex is now characterized by the property that the map of a loop in R^2 onto the manifold of the field is not smoothly contractible. As a consequence there is at least one singularity of the field inside such a loop. In statistical mechanics, vortices have been mainly discussed in relation with the two dimensional XY model. The classical energy of a vortex is given by $E \approx \pi \ln(R/a)$ where R is the size of the vortex. Based on the simple energy versus entropy argument that the free energy is given by $F=E-TS$ with $S=2\ln(R/a)$, Kosterlitz and Thouless [31] inferred the occurrence of a phase transition at $T=\pi/2$.

This argument does rely on the assumptions that the free energy of a vortex at a fixed location is essentially given by its energy and that knowledge of the free energy of an isolated vortex is sufficient to determine the critical properties of the system. The possibility of a Kosterlitz-Thouless-(KT) type transition occurring also in non-Abelian models has been suggested by Solomon *et al.* [32]. It has been argued that the free energy of a vortex at a fixed location is bounded as $R\to\infty$ for non-Abelian theories [33] and so a simple KT style analysis cannot be carried out. However, it has also been suggested [34,33] that for non-Abelian theories the interaction between vortices is such that the free energy of multivortex configurations cannot be inferred from the properties of an isolated vortex. It is clear that further studies are necessary to clarify the true position.

A number of approaches can be taken.

(i) The free energy of an isolated vortex can be calculated at least in one-loop perturbation theory and in a lattice simulation to check that the argument above can be made. Also the free energy of multivortex configurations should be computed by simulation.

(ii) The vortices of SO(N) can be suppressed by eliminating any configuration which contains one or more vortices. The finite-size scaling analysis can be repeated to see whether the continuum theory is more readily observed.

(iii) The matrix models based on Spin(N) can be simulated and compared with the SO(N) models and the mass ratios predicted from the exact S matrix can be computed.

(iv) Study (a) the RP^{N-1} model with action

$$S(\sigma,\mathbf{s}) = \beta \sum_{x,t} \sigma_1(x,t)\mathbf{s}(x,t)\cdot\mathbf{s}(x+1,t) + \sigma_2(x,t)\mathbf{s}(x,t)\cdot\mathbf{s}(x,t+1) - \ln(z)\sum_{\text{plaquettes}} P(\sigma), \tag{7.2}$$

where $\mathbf{s}$ is an N-component vector of unit length, σ_μ, $\mu=1,2$ is a gauge field taking values in $[1,-1]$, and $P(\sigma)$ signifies the plaquette and (b) the model whose manifold has the same topology as the SO(4) manifold but in which the vortex operators can be explicitly constructed. This model has action

$$S(\sigma,\mathbf{s},\mathbf{r}) = \beta \sum_{x,t} \sigma_1(x,t)\big(\mathbf{s}(x,t)\cdot\mathbf{s}(x+1,t) + \mathbf{r}(x,t)\cdot\mathbf{r}(x+1,t)\big) + \sigma_2(x,t)\big(\mathbf{s}(x,t)\cdot\mathbf{s}(x,t+1) + \mathbf{r}(x,t)\cdot\mathbf{r}(x,t+1)\big) - \ln(z)\sum_{\text{plaquettes}} P(\sigma), \tag{7.3}$$

where $\mathbf{s}$ and $\mathbf{r}$ are four-component vectors of unit length and σ_μ and $P(\sigma)$ are as defined in (a). In both models the renormalization group flow in (β,z) can be studied using Monte Carlo methods and hence the effect of vortices, measured by $P(\sigma)$ and controlled by the fugacity, z, can be determined.

These projects are currently in hand.

The outcome is that we should be wary of claims that the continuum theory has been observed which are based on the observation of scaling in a limited window in the coupling constant. Even if properties of the continuum are observed at short distances it does not follow that observables on the scale of the correlation length, which are sensitive to so-called nonperturbative effects, are controlled by the continuum theory. This could be the case for any lattice model which has nontrivial topological artifacts. It has been pointed out [32] that QCD is such a theory since the gauge group is $\mathrm{SU}(3)/Z_3$ where Z_3 is the center of SU(3) [35]. It is important to determine whether such an effect exists in QCD and at what level of accuracy it needs to be taken into account in present-day simulations. We have been unable to observe any continuum properties in the SO(N) matrix models but it remains to be seen whether Spin(N) models have the same problems.

ACKNOWLEDGMENTS

We wish to thank Dr. I. T. Drummond, Dr. F. Niedermayer, and Professor U. Wolff for useful discussions and advice. We also wish to thank the Leverhulme Trust for a grant to support this work. R.R.H. thanks the Royal Society for a research grant for equipment on which much of the computer simulation was done.

[1] T. J. Hollowood, Phys. Lett. B **329**, 450 (1994).
[2] M. Lüscher, P. Weisz, and U. Wolff, Nucl. Phys. **B359**, 221 (1991).
[3] A. B. Zamolodchikov and Al. B. Zamolodchikov, Ann. Phys. (N.Y.) **120**, 25 (1979).
[4] A. M. Polyakov and P. B. Wiegmann, Phys. Lett. B **131**, 121 (1983).
[5] E. Ogievetsky *et al.*, Nucl. Phys. **B280** [FS18], 45 (1987).
[6] P. Hasenfratz and F. Niedermeyer, Phys. Lett. B **245**, 529 (1990).
[7] P. Hasenfratz, M. Maggiore, and F. Niedermeyer, Phys. Lett. B **245**, 522 (1990).
[8] P. Rossi and E. Vicari, Phys. Rev. D **49**, 1621 (1994).
[9] I. T. Drummond and R. R. Horgan, Phys. Lett. B **321**, 246 (1994).
[10] U. Wolff, Phys. Lett. B **248**, 335 (1990).

[11] U. Wolff, Nucl. Phys. **B334**, 581 (1990).
[12] U. Wolff, Phys. Lett. B **222**, 473 (1989).
[13] S. Caracciolo *et al.*, in *Lattice '92*, Proceedings of the International Symposium, Amsterdam, the Netherlands, edited by J. Smit and P. van Baal [Nucl. Phys. B (Proc. Suppl) **30**, 815 (1993)].
[14] S. Caracciolo *et al.*, Phys. Rev. Lett. **71**, 3906 (1993).
[15] S. Caracciolo *et al.*, in *Lattice '93*, Proceedings of the International Symposium, Dallas, Texas, edited by T. Draper *et al.* [Nucl. Phys. B (Proc. Suppl.) **34**, 129 (1994)].
[16] M. Hasenbusch, Phys. Rev. D **53**, 3445 (1996).
[17] N. Niedermayer, P. Weisz, and Dong-Shin Shin, Phys. Rev. D (to be published).
[18] G. Parisi, in *High Energy Physics–1980*, Proceedings of the 20th International Conference, Madison, Wisconsin, edited by L. Durand and L. Pondrom, AIP Conf. Proc. No. 68 (AIP, New York, 1981).
[19] T. J. Hollowood (private communication).
[20] J. Shigemitsu and J. B. Kogut, Nucl. Phys. **B190** [FS3], 365 (1981).
[21] P. Hasenfratz and F. Niedermayer, Z. Phys. B **92**, 91 (1993).
[22] I. T. Drummond, S. Duane, and R. R. Horgan, Nucl. Phys. **B220**, 119 (1983).
[23] M. Lüscher, Phys. Lett. **118B**, 391 (1982).
[24] M. Hasenbusch and S. Meyer, Phys. Rev. D **45**, 4376 (1992).
[25] S. L. Adler, Phys. Rev. D **23**, 2901 (1981).
[26] R. Gupta *et al.*, Phys. Rev. Lett. **68**, 1996 (1988).
[27] M. Hasenbusch and S. Meyer, Phys. Rev. Lett. **68**, 435 (1992).
[28] M. Creutz, Phys. Rev. Lett. **50**, 1411 (1983).
[29] M. Hasenbusch, in *Lattice '94*, Proceedings of the International Symposium, Bielefeld, Germany, edited by F. Karsch *et al.* [Nucl. Phys. B (Proc. Suppl.) **42**, 764 (1995)].
[30] M. Gourdin, *Basics of Lie Groups* (Éditions Frontiéres, Gif-sur-Yvette, France, 1982).
[31] J. M. Kosterlitz and D. J. Thouless, J. Phys. C **6**, 1181 (1973).
[32] S. Solomon, Y. Stavans, and E. Domany, Phys. Lett. **112B**, 373 (1982).
[33] A. Sokal (private communication).
[34] F. Niedermayer (private communication).
[35] G. t'Hooft, Nucl. Phys. **B138**, 1 (1978).